PIER C

(Received 30 May 2025, Accepted 4 September 2025, Scheduled 26 September 2025)

Study on Development of Rod-Electrode-Type Microwave Plasma Source at Atmospheric Pressure

Hidenori Sekiguchi*

National Institute of Maritime, Port and Aviation Technology, Mitaka, Tokyo 181-0004, Japan

ABSTRACT: This paper presents a newly developed rod-electrode-type microwave plasma source (MPS), which is mainly composed of a panel mount coaxial connector, a self-made metal adapter with an inlet and outlet of working gas, a quartz tube as a flow path of working gas, and a metal rod-electrode. Microwave energy can be then supplied directly to the working gas from the sharp tip of the metal rod-electrode through the panel mount coaxial connector. To verify the validity of the rod-electrode-type MPS, a reasonable microwave power supply system is built to transmit the microwave power from a magnetron to the panel mount coaxial connector. The experiments demonstrate that the rod-electrode-type MPS can convert by autoignition argon (Ar) into plasma at atmospheric pressure. Moreover, the Ar plasma can be changed to dry air (Air) plasma or nitrogen (N_2) plasma by gradually replacing Ar with Air or N_2. The experimental results show that the rod-electrode-type MPS is potentially an available tool for gas processing at atmospheric pressure.

1. INTRODUCTION

Microwave plasma has the advantages of high electron and gas temperatures, and a wide operating pressure range [1]. It has been already used in many industries requiring surface treatment and modification, ozone generation, gaseous treatment, antibacterial treatment, etc. [2]. In recent years, microwave plasma is expected to be applied to gas processing such as the decomposition of greenhouse gases (GHGs) and the reforming of gas fuels, in terms of the reduction of GHG emissions [3–9].

So far, microwave plasma sources (MPSs) have been mainly developed with two microwave power supply types: waveguide-supplied MPSs and coaxial-line-supplied MPSs [10, 11]. Waveguide-supplied MPS has high potential for gas processing such as the decomposition of gaseous pollutants (mainly volatile organic compounds (VOCs)) of relatively high concentration (up to 100%) in the working gas and the reforming of methane for hydrogen production. However, the design and structure are complex to optimally focus electric field at the discharge region in the waveguide [12]. Moreover, waveguide-supplied MPSs need high input microwave power to ignite and maintain the microwave plasma at atmospheric pressure. On the other hand, coaxial-line-supplied MPSs can easily transmit microwave power to themselves using a coaxial cable, but the generated plasma region is small such as a micro-plasma [11]. As a conclusion, the coaxial-line-supplied MPS with a larger plasma region would be useful to widely apply microwave plasma for gas processing at atmospheric pressure.

In this study, a rod-electrode-type MPS, which is a kind of coaxial-line-supplied MPS, has been newly developed for gas processing at atmospheric pressure [13, 14]. The rod-electrode-type MPS was mainly composed of a panel mount coaxial connector, a self-made metal adapter with an inlet and outlet of working gas, a quartz tube as a flow path of working gas, and a metal rod-electrode. As explained in Section 2 below, the working gas can flow around the metal rod-electrode covered with quartz tube in the simple structure and easy assembly. The microwave energy can be then supplied directly to the working gas from the sharp tip of the metal rod-electrode through the panel mount coaxial connector.

This paper first presents the newly developed rod-electrode-type MPS and a reasonable microwave power supply system. The microwave power supply system is built to transmit microwave power from a magnetron to the rod-electrode-type MPS. Next, the validity of the rod-electrode-type MPS is verified in experiments. The experiments demonstrate that the rod-electrode-type MPS can convert by autoignition argon (Ar) into plasma at atmospheric pressure. Moreover, the Ar plasma can be changed to dry air (Air) plasma or nitrogen (N_2) plasma by gradually replacing Ar with Air or N_2. The plasmas are captured by a digital single-lens reflex (DSLR) camera with a complementary metal oxide semiconductor (CMOS) image sensor, and the emission spectra are measured by a spectrometer with a charge-coupled device (CCD) image sensor. In addition, plasma shapes are investigated for the length and tip angle of the rod-electrode, the flow rate of the working gas, and the average transmission power. The experimental results show that the rod-electrode-type MPS is potentially an available tool for gas processing at atmospheric pressure.

2. EXPERIMENT

2.1. Rod-Electrode-Type MPS

Figure 1 shows the structure diagram and photograph of a developed rod-electrode-type MPS, which consists mainly of rea-

* Corresponding author: Hidenori Sekiguchi (sekiguchi@m.mpat.go.jp).

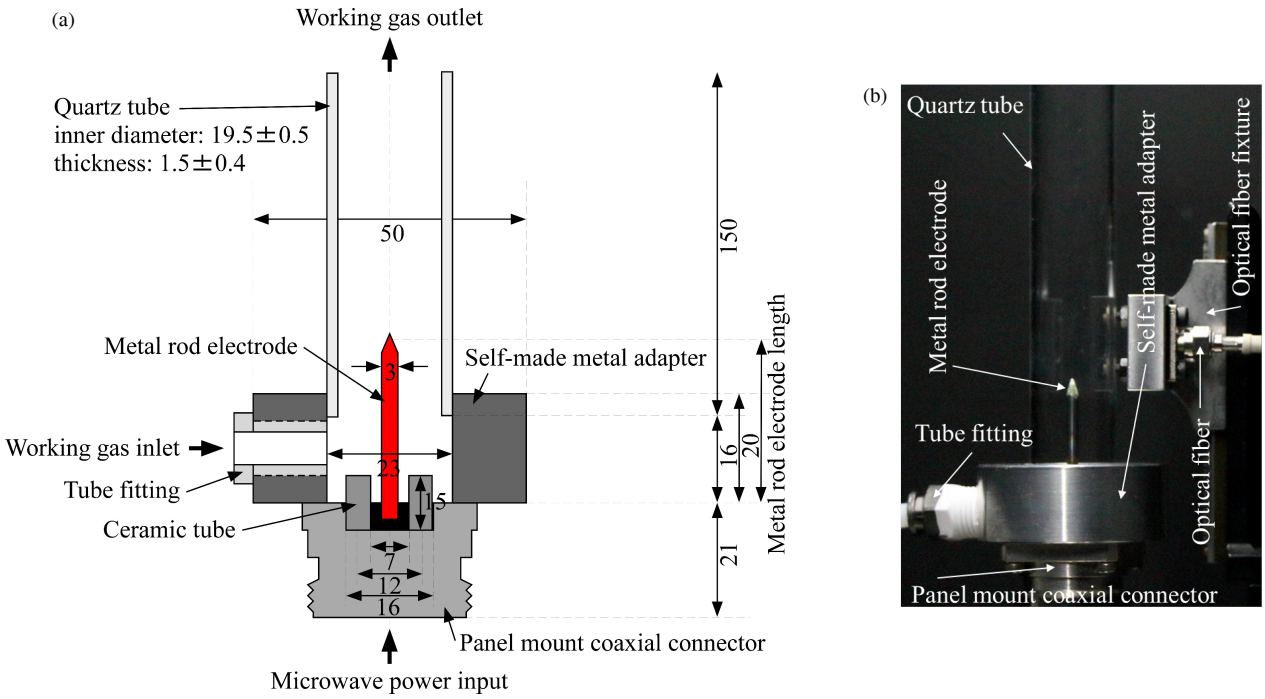

FIGURE 1. Structure diagram and photograph of developed rod-electrode-type MPS. (a) Structure diagram. (b) Photograph.

sonable parts and materials such as a panel mount coaxial connector, a metal rod-electrode, a self-made metal adapter, and a quartz tube. The sizes of the parts and materials are shown in millimeters (mm) in Fig. 1(a). The basic structure and construction can refer to the previous literature [13].

The rod-electrode-type MPS can transmit the microwave power from a coaxial line rather than a waveguide, so it can be installed in a suitable location for actual applications. Further, two or more rod-electrode-type MPSs can be connected in parallel using a coaxial distributor from a microwave power supply system.

2.2. Experimental Setup and Method

Figure 2 shows the schematic diagram of the experimental system. Ar, N_2, and Air were supplied to the rod-electrode-type MPS from each of the industrial gas cylinders. The flow rates were controlled using mass flow controllers (HORIBA, Ltd., SEC-N100 corresponding to each gas).

The microwave power supply system was built using a variable transformer, a microwave oven transformer (MOT), a full wave voltage doubler circuit, a magnetron, and a waveguide-to-coaxial adapter [13, 14]. The magnetron and MOT were for commercial microwave ovens with a power source of a voltage of 100 V and a frequency of 50 Hz. The magnetron had a power rating of 1,000 W with an operation frequency of 2.45 GHz. The MOT was a transformer for its magnetron. The full wave voltage doubler circuit was then build using two high-voltage (HV) capacitors, two HV diodes, and a resistance [13]. As a side note, in order to generate plasma stably using a magnetron, a full wave voltage doubler circuit was more effective than the half wave voltage doubler circuit used widely in commercial microwave ovens, because full wave voltage doubler circuit could generate twice the frequency of the power source. The variable transformer controlled the output power from the magnetron. The waveguide-to-coaxial adapter was reported in detail in the previous literature [13]. The forward and reflection powers at the input port of the rod-electrode-type MPS were calculated using the correction function by the manufacture from the forward and reflection voltages of the digital oscilloscope. The transmission power to the rod-electrode-type MPS was calculated by subtracting the reflection power from the forward power. Incidentally, since the rod-electrode-type MPS can be connected to the waveguide-to-coaxial adapter using a coaxial cable, it can also be installed in a suitable location away from the microwave power supply system.

The experiments were conducted in a darkroom to observe the emission of light by plasmas. The plasma was captured by a DSLR camera, and the emission spectrum of the plasma was measured by a spectrometer with an optical fiber. The DSLR camera and spectrometer, including their setup parameters, were reported in detail in the previous literature [13]. The optical fiber head was then set at a 10 mm upper distance and 30 mm horizontal distance from the sharp tip of the metal rod-electrode.

3. RESULTS AND DISCUSSION

3.1. Initial Experiments

Noble gases such as Ar are well known to be easily converted into plasma. So, in the initial experiments, only Ar was fed into the rod-electrode-type MPS at atmospheric pressure. In Fig. 2, when the output power of the magnetron is increased by the variable transformer, the Ar was confirmed to be converted

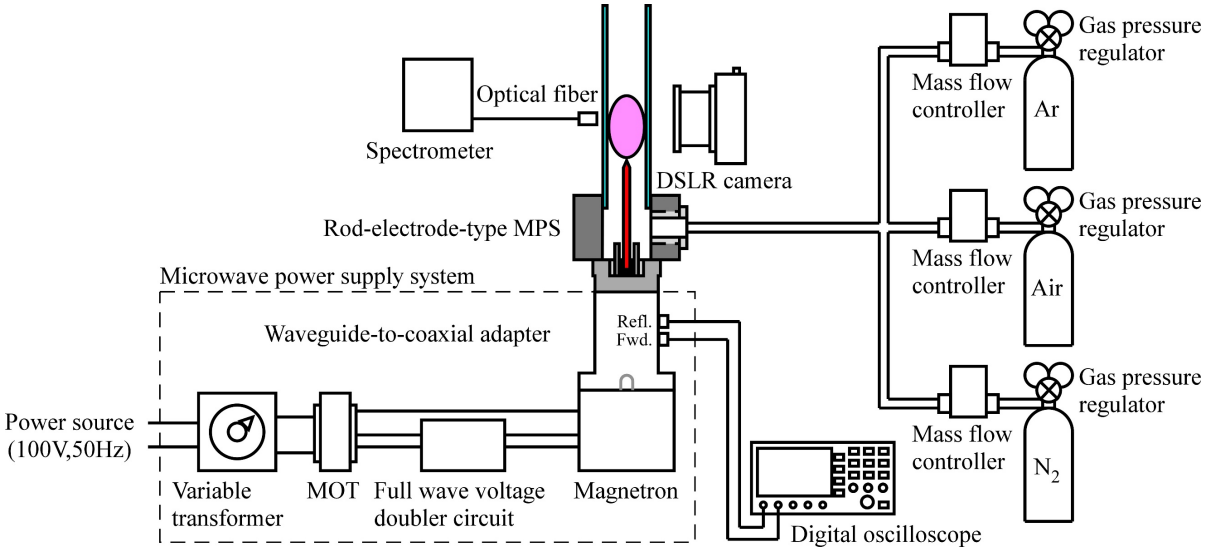

FIGURE 2. Schematic diagram of experimental system.

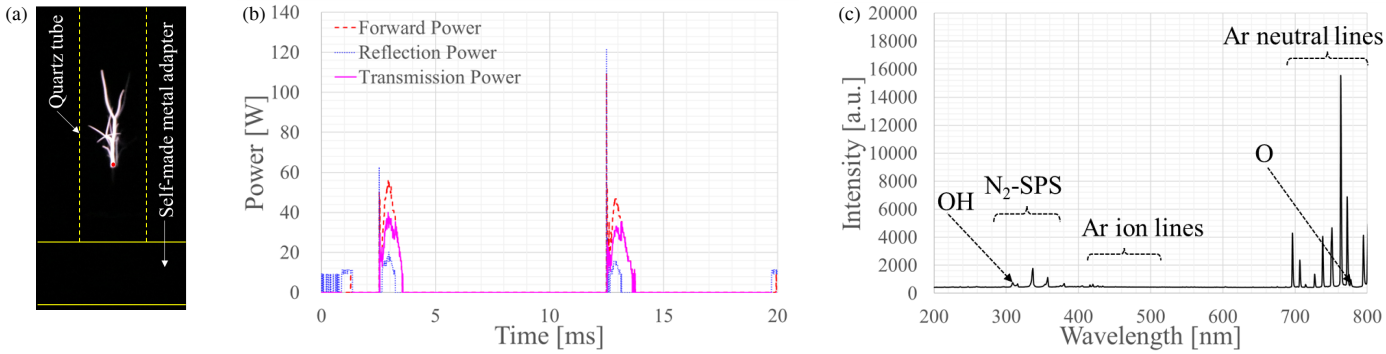

FIGURE 3. Experimental results of Ar plasma at flow rate of 2.5 L/min and average transmission power of approximately 2.1 W. (a) Capture image. (b) Forward, reflection, and transmission power waveforms at input port of rod-electrode-type MPS. (c) Emission spectrum.

into plasma by autoignition from the sharp tip of the metal rod-electrode. Additionally, Ar plasma could be generated at the flow rates of 0.5–10 L/min and metal rod-electrode lengths of approximately 20–50 mm. The output power of the magnetron after generating the Ar plasma could be reduced to some extent while maintaining the Ar plasma.

On the other hand, rod-electrode-type MPS was difficult to convert by autoignition N_2 and Air into plasma at atmospheric pressure. However, N_2 and Air plasmas could be changed from Ar plasma, by gradually replacing Ar with N_2 and Air, respectively. Specifically, Ar was first converted into plasma in the rod-electrode-type MPS. Next, N_2 or Air was fed into the Ar plasma, and Ar/N_2 or Ar/Air plasma was generated with the mixed gas of Ar and N_2 or Air. Finally, Ar was interrupted into the Ar/N_2 or Ar/Air plasma, and only N_2 or Air could be converted into plasma in the rod-electrode-type MPS.

3.2. Ar Plasma

Figure 3 shows experimental results of the Ar plasma at the flow rate of 2.5 L/min. Figs. 3(a), (b), and (c) show the capture image, corrected forward, reflection, and transmission power waveforms at the input port of the rod-electrode-type MPS, and the emission spectrum, respectively. The rod-electrode-type MPS had then the metal rod-electrode length of approximately 36 mm from the top surface of the panel mount coaxial connector in Fig. 1(a).

In Fig. 3(a), the dashed and solid lines show the outlines of the quartz tube and self-made metal adapter, respectively. The red point indicates the location of the sharp tip of the metal rod-electrode. From Fig. 3(a), the Ar plasma like streamer discharge can be confirmed to generate from the sharp tip of the metal rod-electrode. In fact, it appeared to fluctuate, and might be caused by the gas characteristics of Ar. The extension of the Ar plasma above the sharp tip of the metal rod-electrode will be the effect of the gas flow in the upward direction.

In Fig. 3(b), the forward, reflection, and transmission power waveforms will be mainly affected by the electrical characteristics of the Ar plasma and experimental system. Here, electrical characteristics of the Ar plasma indicate the degree of ionization or the characteristic impedance in the Air plasma. The maximum transmission power was then about 30–40 W with the frequency of 100 Hz, which was generated by the full wave

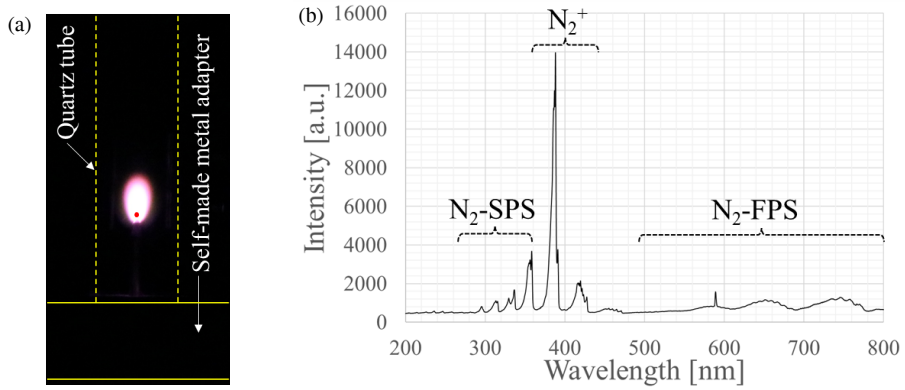

FIGURE 4. Experimental results of N_2 plasma at flow rate of 1.0 L/min and average transmission power of approximately 133.3 W. (a) Capture image. (b) Emission spectrum.

voltage doubler circuit in the experimental system. The average transmission power and efficiency were then approximately 2.1 W and 60.0%, respectively.

In Fig. 3(c), some peaks were observed by the Ar plasma. The large and small emission peaks in the wavelength ranges of approximately 695–800 nm and 410–520 nm result from Ar neutral lines (Ar I) and Ar ion lines (Ar II), respectively [15–18]. Namely, the Ar in the rod-electrode-type MPS could be converted into plasma at atmospheric pressure. Besides, the emission peaks in the wavelength range of approximately 280–370 nm may be caused by the second positive system of nitrogen molecule (N_2-SPS). The emission peaks at the wavelengths of 309 nm and 777 nm may be caused by hydroxyl radical (OH) and atomic oxygen (O), respectively. These emission peaks of the N_2-SPS, OH, and O in the Ar plasma will result from the impurities in the industrial Ar gas cylinder [16, 17]. By the way, the emission spectrum does not correspond to the capture image in Fig. 4(a), because the general DSLR camera with a CMOS image sensor has a high spectral sensitivity in wavelengths of approximately 400–700 nm.

In this subsection, the rod-electrode-type MPS showed to be convertible Ar into plasma by autoignition at atmospheric pressure.

3.3. N_2 Plasma

Figure 4 shows experimental results of the N_2 plasma at the flow rate of 1.0 L/min and the average transmission power of approximately 133.3 W, which was generated by using the rod-electrode-type MPS with the metal rod-electrode length of approximately 40 mm. The average transmission efficiency was then 68.7%. Figs. 4(a) and (b) show the capture image and emission spectrum, respectively.

In Fig. 4(a), the N_2 plasma like a flame or candle can be confirmed to generate from the sharp tip of the metal rod-electrode in the quartz tube. In fact, it appeared very stable. The visible shape was apparently different from that of the Ar plasma, and the N_2 plasma seemed to operate as the diffuse discharge due to gas characteristics of the N_2.

The average transmission power was larger than that of the Ar plasma, in order to maintain the N_2 plasma. The average transmission efficiency was higher that of the Ar plasma and will be affected by the degree of ionization or the characteristic impedance in the N_2 plasma.

In Fig. 4(b), two large emission peaks in the wavelength range of approximately 370–450 nm result from the first negative system of nitrogen molecular ion (N_2^+) [19]. Some emission peaks in the wavelength range of approximately 280–370 nm result from the N_2-SPS. The small emission peaks in the wavelength range of approximately 500–800 nm are caused by the first positive system of nitrogen molecule (N_2-FPS). Namely, the N_2 could be converted into plasma in the rod-electrode-type MPS at atmospheric pressure.

Here, the length of the metal rod-electrode was investigated in the N_2 plasma. Fig. 5 shows the capture images of the N_2 plasma using the rod-electrode-type MPS with the metal rod-electrode lengths of approximately 30, 40, and 50 mm at the flow rate of 1.0 L/min and the average forward power of roughly 205 W. The visible shape of the N_2 plasma was reduced with increasing the metal rod-electrode length. The average transmission power decreased from 168.7 W with the metal rod-electrode length of approximately 30 mm to 121.8 W with the metal rod-electrode length of approximately 50 mm. Namely, the average reflection power increased with increasing

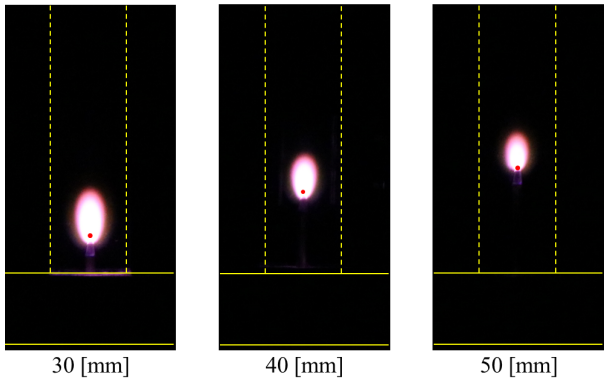

FIGURE 5. Capture images of N_2 plasma using rod-electrode-type MPS with metal rod-electrode lengths of approximately 30, 40, and 50 mm at flow rate of 1.0 L/min and average forward power of roughly 205 W.

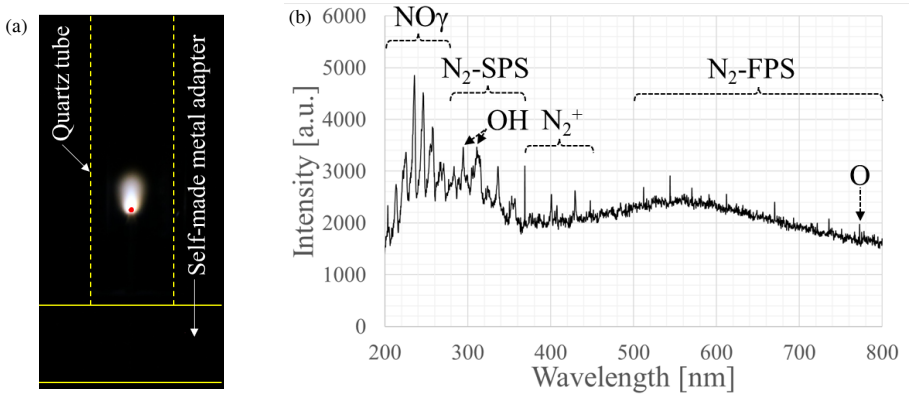

FIGURE 6. Experimental results of Air plasma at flow rate of 1.0 L/min and average transmission power of approximately 58.9 W. (a) Capture image. (b) Emission spectrum.

the metal rod-electrode length. The average transmission efficiency decreased then from 82.4% with the metal rod-electrode length of approximately 30 mm to 55.8% with the metal rod-electrode length of approximately 50 mm. Ultimately, the reduction in the visible shape of the N_2 plasma was caused by the decrease in the average transmission power with increasing the metal rod-electrode length. The metal rod-electrode length in the rod-electrode-type MPS was confirmed to have a large effect on the average transmission efficiency to the rod-electrode-type MPS.

Besides, the tip angle of the metal rod-electrode in the rod-electrode-type MPS was investigated in the N_2 plasma. The N_2 plasma was generated using the rod-electrode-type MPS with the metal rod-electrode length of approximately 40 mm and the tip angles about 28, 44, 51, 67, and 90 degrees. The tip angle of the metal rod-electrode was then confirmed to have little effect on the visible shape of the N_2 plasma and average transmission efficiency, although the experimental results were not shown here.

In this subsection, the rod-electrode-type MPS showed to be able to stably convert N_2 into plasma by autoignition at atmospheric pressure. Additionally, the length of the metal rod-electrode in the rod-electrode-type MPS had a large effect on the average transmission efficiency to the rod-electrode-type MPS, whereas the tip angle of the metal rod-electrode had little effect on the average transmission efficiency.

3.4. Air Plasma

Figure 6 shows the experimental results of the Air plasma at the flow rate of 1.0 L/min and the average transmission power of approximately 58.9 W, which was generated by using the rod-electrode-type MPS with the metal rod-electrode length of approximately 42 mm. The average transmission efficiency was then 59.6%. Figs. 6(a) and (b) show the capture image and emission spectrum, respectively.

In Fig. 6(a), the Ar plasma like a small flame or candle can be confirmed to generate from the sharp tip of the metal rod-electrode in the quartz tube. In fact, it appeared very stable, similar to N_2 plasma. The visible shape was also apparently different from that of Ar plasma, and Air plasma seemed to operate as the diffuse discharge due to gas characteristics of the Air. In addition, the sharp tip of the metal rod-electrode was red-hot, which may be caused by the oxidation reaction of the sharp tip surface of the metal rod-electrode.

The average transmission power was larger than that of Ar plasma and smaller than that of N_2 plasma, in order to maintain the Air plasma. The average transmission efficiency was comparable to that of Ar plasma and lower than that of N_2 plasma. It will be affected by the degree of ionization or the characteristic impedance in the Air plasma.

In Fig. 6(b), the large emission peaks in the wavelength ranges of approximately 200–280 nm result from the gamma band system of nitric oxide molecule (NOγ). Besides, some small emission peaks in the wavelength ranges of approximately 280–370 nm, 370–450 nm, and 500–800 nm result from the N_2-SPS, N_2^+, and N_2-FPS, respectively. The emission peak at the wavelength of 777 nm will be caused by O. These emission peaks of the NOγ, N_2-SPS, N_2^+, N_2-FPS, and O are also observed by Air plasma in the literature [19, 20]. On the other hand, the emission peaks at the wavelengths of 295 and 309 nm will be caused by OH. The OH may result from the hydrogen (H_2) and hydrogen oxide (H_2O) as impurities in the industrial Air gas cylinder. The noteworthy points were that N_2 and oxygen molecules (O_2) in the Air could be ionized and dissociated by the Air plasma. In particular, the presence of emissions from NOγ implied the production of nitric oxide molecules (NO). In addition, an ozone (O_3) odor was present in the exhaust gas after the Air plasma.

Here, the flow rate and average transmission power were investigated in the Air plasma. Figs. 7(a) and (b) show the capture images of the Air plasma at flow rates of 0.5, 1.0, 1.5, and 2.0 L/min and the average forward power of roughly 127 W, and at the flow rate of 1.0 L/min, respectively and the average transmission powers of approximately 58.9, 76.8, 95.0, and 110.4 W.

In Fig. 7(a), the width of the Air plasma decreased with increasing the flow rate, whereas the length of the Air plasma was not significantly affected by the change in the flow rate. The increase in the flow rate leads to the increase in the flow velocity in the upward direction in the quartz tube. The increase

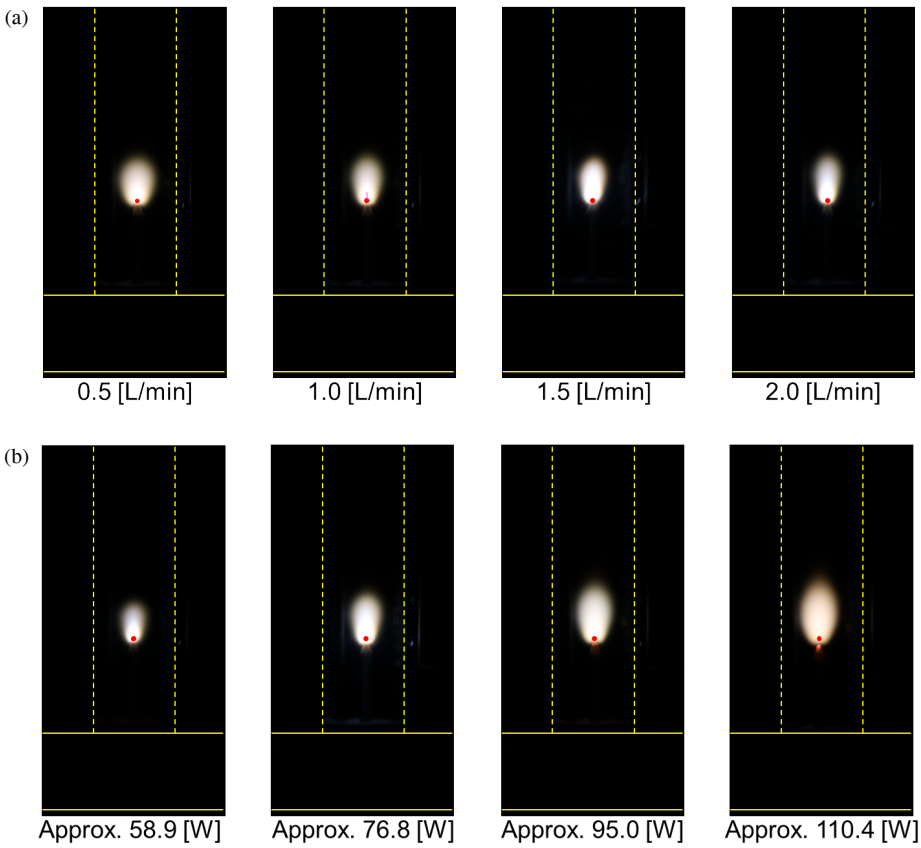

FIGURE 7. Capture images of Air plasma. (a) At flow rates of 0.5, 1.0, 1.5, and 2.0 L/min and average forward power of roughly 127 W. (b) At flow rate of 1.0 L/min and average transmission powers of approximately 58.9, 76.8, 95.0, and 110.4 W.

in the flow velocity decreases the microwave energy per unit time supplied to the Air and extends the Air plasm in the upward direction. The average transmission power increased then slightly with increasing the flow rate. Accordingly, the average transmission efficiency also increased slightly from 56.3% at the flow rate of 0.5 L/min to 58.3% at the flow rate of 2.0 L/min. The average transmission efficiency will be affected by the degree of ionization or the characteristic impedance in the Air plasma.

In Fig. 7(b), the width and length of the Air plasma extended with increasing the average transmission power. The extension of the Air plasma will be caused by the increase in the microwave energy per unit time supplied to the Air flowing in the quartz tube. The average transmission efficiency increased then slightly from 59.6% at the average transmission power of approximately 58.9 W to 63.0% at the average transmission power of approximately 110.4 W. The increase in the average transmission power leads to the extension of the Air plasma. On the other hand, the increase in the average transmission power should to be careful to increase the red-hot zone on the sharp tip of the metal rod-electrode.

In this subsection, the rod-electrode-type MPS showed to be able to stably convert Air into plasma at atmospheric pressure. In the emission spectrum, the presence of the emissions from NOγ implied the production of NO. Moreover, an ozone (O_3) odor was present in the exhaust gas after the Air plasma. Thus, the rod-electrode-type MPS could be potentially an available tool for gas processing at atmospheric pressure. Additionally, the visible shape and average transmission efficiency of the Air plasma were slightly affected by the flow rate and average transmission power, and will be caused by the degree of ionization or the characteristic impedance in the Air plasma.

4. CONCLUSION

This paper has presented a newly developed rod-electrode-type MPS and microwave power supply system. The rod-electrode-type MPS showed to be simple in structure and easy to assemble. It can be installed in a suitable location for actual applications, by connecting to the microwave power supply system using a coaxial cable.

In the experiments, the rod-electrode-type MPS could be converted by autoignition Ar into the plasma by increasing the average transmission power. Moreover, Ar plasma could be changed to N_2 plasma or Air plasma by gradually replacing Ar with N_2 or Air. The type of gas affected the plasma shape, the average transmission efficiency, and thus the degree of ionization or the characteristic impedance in the plasma. In particular, the experimental results of the Air plasma implied the production of NO and O_3. Consequently, the rod-electrode-type MPS was demonstrated to be potentially an available tool for gas processing at atmospheric pressure.

In addition, the length of the metal rod-electrode had a large effect on the plasma shape, the average transmission efficiency, and thus the degree of ionization or the characteristic impedance in the plasma. In contrast, the tip angle of the metal rod-electrode had little effect on them. Besides, the flow rate of the working gas and average transmission power to the rod-electrode-type MPS had a small effect on them. In order to effectively apply the rod-electrode-type MPS to gas processing at atmospheric pressure, the improvement of the rod-electrode MPS will be necessary for increasing the plasma region in the flow path of the working gas and the average transmission efficiency to the rod-electrode-type MPS. In the near future, the improved rod-electrode-type MPS will be applied to gas processing such as the decomposition of GHGs and the reforming of gas fuels, in terms of the reduction of GHG emissions.

ACKNOWLEDGEMENT

This work was supported in part by the Japan Society for the Promotion of Science (JSPS) KAKENHI Grant Number 21K04521.

REFERENCES

[1] Fridman, A., *Plasma Chemistry*, Cambridge University Press, 2008.

[2] Fridman, A. and L. A. Kennedy, *Plasma Physics and Engineering*, CRC Press, 2004.

[3] Bogaerts, A. and G. Centi, "Plasma technology for CO_2 conversion: A personal perspective on prospects and gaps," *Frontiers in Energy Research*, Vol. 8, 111, 2020.

[4] Qin, Y., G. Niu, X. Wang, D. Luo, and Y. Duan, "Status of CO_2 conversion using microwave plasma," *Journal of CO_2 Utilization*, Vol. 28, 283–291, 2018.

[5] Yin, Y., T. Yang, Z. Li, E. Devid, D. Auerbach, and A. W. Kleyn, "CO_2 conversion by plasma: how to get efficient CO_2 conversion and high energy efficiency," *Physical Chemistry Chemical Physics*, Vol. 23, No. 13, 7974–7987, 2021.

[6] Kiefer, C. K., R. Antunes, A. Hecimovic, A. Meindl, and U. Fantz, "CO_2 dissociation using a lab-scale microwave plasma torch: An experimental study in view of industrial application," *Chemical Engineering Journal*, Vol. 481, 148326, 2024.

[7] Choi, D. H., S. M. Chun, S. H. Ma, and Y. C. Hong, "Production of hydrogen-rich syngas from methane reforming by steam microwave plasma," *Journal of Industrial and Engineering Chemistry*, Vol. 34, 286–291, 2016.

[8] Jasiński, M., M. Dors, H. Nowakowska, G. V. Nichipor, and J. Mizeraczyk, "Production of hydrogen via conversion of hydrocarbons using a microwave plasma," *Journal of Physics D: Applied Physics*, Vol. 44, No. 19, 194002, 2011.

[9] Jasiński, M., D. Czylkowski, B. Hrycak, M. Dors, and J. Mizeraczyk, "Atmospheric pressure microwave plasma source for hydrogen production," *International Journal of Hydrogen Energy*, Vol. 38, No. 26, 11 473–11 483, 2013.

[10] Mizeraczyk, J., M. Jasinski, M. Dors, and Z. Zakrzewski, "Microwave plasma sources for gas processing," in *AIP Conference Proceedings*, Vol. 993, No. 1, 287–294, 2008.

[11] Mizeraczyk, J., M. Jasiński, H. Nowakowska, and M. Dors, "Studies of atmospheric-pressure microwave plasmas used for gas processing," *Nukleonika*, Vol. 57, No. 2, 241–247, 2012.

[12] Deng, P., W. Xiao, F. Wang, and Z. Zhang, "Design of a novel microwave plasma source based on ridged waveguide," *Progress In Electromagnetics Research Letters*, Vol. 101, 19–27, 2021.

[13] Sekiguchi, H., "Pure ammonia direct decomposition using rod-electrode-type microwave plasma source," *International Journal of Hydrogen Energy*, Vol. 57, 1010–1016, 2024.

[14] Sekiguchi, H., "Experimental investigations of plasma-assisted ammonia combustion using rod-electrode-type microwave plasma source," *International Journal of Hydrogen Energy*, Vol. 65, 66–73, 2024.

[15] Kramida, A., Y. Ralchenko, J. Reader, and N. A. Team, "Nist atomic spectra database (ver. 5.9)," National Institute of Standards and Technology, 2021.

[16] Hoentsch, M., R. Bussiahn, H. Rebl, C. Bergemann, M. Eggert, M. Frank, T. V. Woedtke, and B. Nebe, "Persistent effectivity of gas plasma-treated, long time-stored liquid on epithelial cell adhesion capacity and membrane morphology," *PLoS One*, Vol. 9, No. 8, e104559, 2014.

[17] Liu, J.-R., G.-M. Xu, X.-M. Shi, and G.-J. Zhang, "Low temperature plasma promoting fibroblast proliferation by activating the NF-κB pathway and increasing cyclinD1 expression," *Scientific Reports*, Vol. 7, No. 1, 11698, 2017.

[18] Bogaerts, A., R. Gijbels, and J. Vlcek, "Modeling of glow discharge optical emission spectrometry: Calculation of the argon atomic optical emission spectrum," *Spectrochimica Acta Part B: Atomic Spectroscopy*, Vol. 53, No. 11, 1517–1526, 1998.

[19] Deng, X. L., A. Y. Nikiforov, P. Vanraes, and C. Leys, "Direct current plasma jet at atmospheric pressure operating in nitrogen and air," *Journal of Applied Physics*, Vol. 113, No. 2, 023305, 2013.

[20] Khalili, F., B. Shokri, M.-R. Khani, M. Hasani, F. Zandi, and A. Aliahmadi, "A study of the effect of gliding arc non-thermal plasma on almonds decontamination," *AIP Advances*, Vol. 8, No. 10, 105024, 2018.